

Space-resolved investigation of soft-x-ray emission characteristics of a laser plasma in a half-cylindrical shell target

Yao-lin Li, Zhi-zhan Xu, Shi-sheng Chen, Xiao-fang Wang,
Zhi-ming Jiang, and Xian-ping Feng

Shanghai Institute of Optics and Fine Mechanics, P.O. Box 8211, Shanghai, People's Republic of China

(Received 1 May 1989; revised manuscript received 13 December 1989)

Results are presented of experimental research aimed at the study of hydrodynamic processes and soft-x-ray (SXR) emission characteristics of a laser-produced plasma in a half-cylindrical-shell target. Experimental measurements show that this kind of target can effectively increase the short-wavelength SXR emission of the laser-produced plasma in the grooved region.

In experimental research of laser plasmas, targets of various geometries are used for different purposes such as the inertial confined fusion (ICF) and the x-ray laser (XRL). Up to now, numbers of results are published for targets in varieties of geometries,¹⁻³ and target designing has now become a very important branch in both fields of ICF and XRL research.^{4,5}

In this paper, we report the experimental results of soft-x-ray (SXR) emission from a half-cylindrical-shell target by using a pinhole transmission grating (PTG) spectrometer. Measurements show that this kind of target can effectively converge the plasmas and then enhance the short-wavelength SXR emission in the concave region.

Experiments are performed on the Six-Beam Nd:glass Laser Facility in the Shanghai Institute of Optics and Fine Mechanics.⁶ The schematic setup of the experiment is shown in Fig. 1. The laser wavelength is $1.06\ \mu\text{m}$, and pulse duration is 300 ps. Two beams of the facility are combined into one and focused to a $2\ \text{mm} \times 100\ \mu\text{m}$ line on the target surface, with a corresponding intensity of about $10^{13}\ \text{W}/\text{cm}^2$.

The targets used in the experiment are dented into the shape similar to a half-cylindrical groove with thick foils (about $100\ \mu\text{m}$ thick) of aluminum or copper, of which the diameter of the groove is approximately $200\text{--}300\ \mu\text{m}$. The laser beam is focused to the inner surface with the

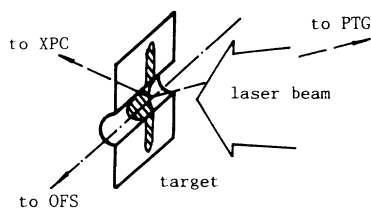


FIG. 1. The schematic setup of the experiment. XPC is the x-ray pinhole camera; PTG is the pinhole transmission grating spectrometer; and OFS is the optical framing system positioned on the groove axis. The PTG is 37° to the normal of the target plane, with the grating bars parallel to the focusing line.

focusing line perpendicular to the axis of the groove to ensure a uniform irradiation across the groove. Planar targets of both material are also used for comparisons.

The space-resolving PTG (Ref. 7) is positioned 37° off the laser beam, with the grating bars parallel to the focusing line to give a spatial resolution across the groove. Its pinhole diameter and grating period are 50 and $1\ \mu\text{m}$, respectively. With the typical arrangement and irradiation condition, the spectral resolution and the spatial resolution of the PTG are $2\ \text{\AA}$ and $60\ \mu\text{m}$, respectively.

We use the modified 5F medical x-ray film for our data recording. This film has nominally the same structure parameters as those of the Kodak SB-392 (see Table I). According to Henke *et al.*,⁸ two types of films that share the same structure parameters should have a similar response character; thus we use their results for our data handling.

We also use a filtered x-ray pinhole camera to monitor the harder x-ray emissions and an on-axis optical framing system to study the temporal and spatial evolution of the coronal plasma (see Fig. 1).

Figure 2 gives a typical space-resolved spectrum [Fig. 2(a)] of one shot upon Al grooved target by the PTG; its spatial tracings (tracing across the axis of the groove) of two emission lines [Fig. 2(b)] are designated as $K(1s^2-1s2p)$ and $L(2p-3d)$ in Fig. 2(a). Figure 2(a) shows that the SXR emissions from the groove are stronger than those out of the groove, and there are clear boundaries at both edges of the groove along the dispersive direction. In Fig. 2(b), we can see clearly that both the K -line and the L -line emissions have a sudden change

TABLE I. Comparison of Kodak SB-392 film with 5F film.

Film type	Emulsion (μm)	Coating (μm)	Grain size (μm)	AgBr vol. %
5F ^a	8	1	1	0.2
Kodak SB-392 ^b	10	1	1	0.2

^aReference 7.

^bReference 8.

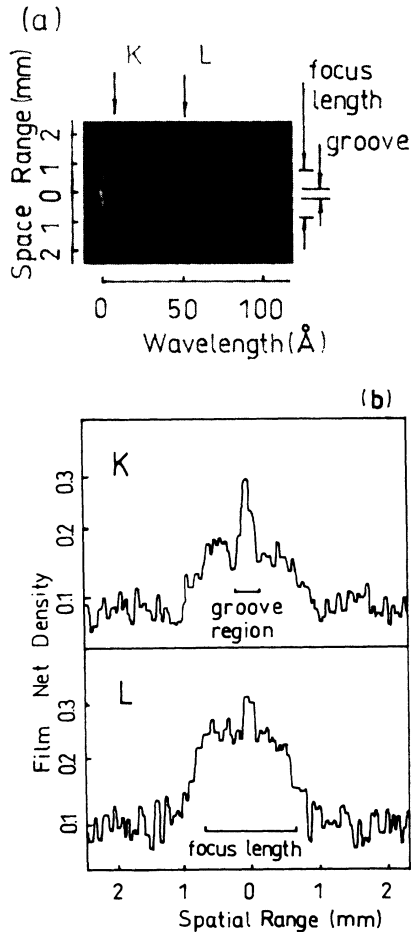


FIG. 2. (a) A typical space-resolved PTG spectrum from a grooved aluminum target. Arrows indicate the tracing locations of the spatial density traces of a K line ($1s^2-1s2p$, 8 \AA) and an L line ($2p-3d$, 52 \AA) in (b). Traces in (b) show large gradients at edges of the groove, and the peak intensity of the K line is much greater than that of the L line (laser energy 21.8 J).

of intensity at the edges of the groove, and form a converging region of high intensity SXR emission in the groove. The convergence shape is quite significant in contrast to the profile out of the groove. Furthermore, the K line (from the Al^{11+} ions) peak is more significant than that of the L line (from the ion Al^{10+} ions).

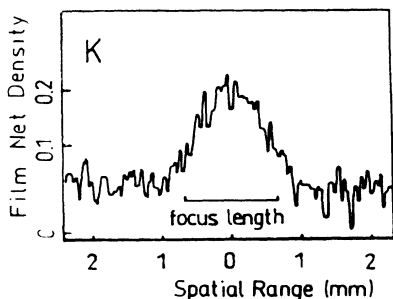


FIG. 3. The spatial traces of an Al K line as mentioned in Fig. 2 of a PTG spectrum for a typical aluminum planar target. There are no intensity gradients within the focusing region. (laser energy 20.7 J)

And, the phenomenon does not exist in the aluminum planar targets. In Fig. 3 we give the spatial traces of the same K line of a typical PTG spectrum of one shot upon a planar target. The steep gradient in Fig. 2(b) does not exist and the profile of the plasma across the focusing region appears similar to a Gaussian distribution, which is supposed to be the transverse profile of the laser beam. Because the irradiation condition of this shot is almost the same as that in Fig. 2, these differences can be attributed only to the different geometries of the targets used.

In the evaluation of the relative intensity by PTG, we set the first order efficiency to be 10% and higher orders are ignored. Figure 4 gives the comparison of the two-line emission intensities of aluminum versus laser energy of grooved targets with those of planar targets. We calculate the peak intensities of the K line [Fig. 4(a)] and the L line [Fig. 4(b)] mentioned above. From the figures, we

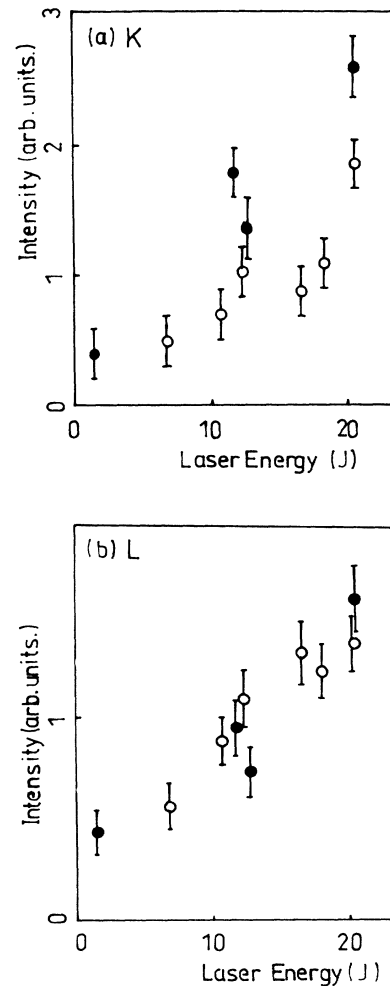


FIG. 4. (a) The K -line ($1s^2-1s2p$) and (b) the L -line ($2p-3d$) peak intensity from aluminum plasmas vs the laser energy. Circles show plane targets; dots show grooved targets. Both figures have the same intensity scale. We can see clearly that the K -line emission increases faster with laser energy for grooved targets than planar, while the L -line emissions remain the same in both cases.

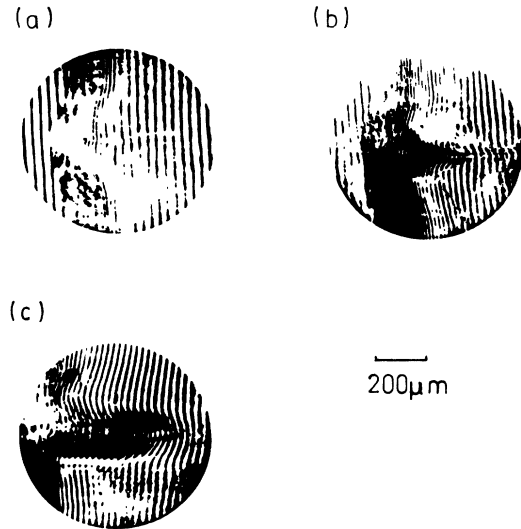


FIG. 5. Typical data of optical framing system from one shot upon an aluminum grooved target. (a) 60 ps before the peak of the laser pulse; (b) 130 ps after the peak of the pulse; (c) 420 ps after the laser pulse peak (laser energy 12.9 J).

can see that the line emission of higher ionized states (K lines from Al^{11+}) from grooved targets is stronger than that from planar targets, while the line emissions from lower ionized states (L lines from Al^{10+}) are almost indistinguishable for both kinds of targets, and this may indicate a higher temperature in grooved cases. And a calculation of copper grooved targets shows that emission increases of the copper grooved targets are not so obvious as that of aluminum ones, and this is probably due to the heavier core mass of the copper ions. It is evident that the groove has an effect on increasing the SXR emissions from ions of higher ionization stages, and this effect is probably stronger for lighter elements than for heavier ones.

From the photographs by the optical framing system of one shot upon an aluminum grooved target in Fig. 5, we can have a physical interpretation of the grooved target effect. The interferential photograph [Fig. 5(a)] shows that the converged plasma appears first at the bottom of the groove when the electron densities within and out of the groove are nearly the same. Then the in-groove plas-

ma grows in the inverse direction of the laser beam at a speed that is twice as large as that of the outer plasma, and the electron density in the grooved region soon surpasses that in the planar region [Fig. 5(b)]. There is no obvious lateral expanding in the in-groove plasma cross to the laser beam. 420 ps after the peak of the laser pulse, the expansion in the laser direction reaches a point about $500 \mu\text{m}$ from the target plane and keeps a rather uniform electron density distribution, while the lateral expansion ends at a maximum of only $200 \mu\text{m}$ [Fig. 5(c)]. On assumption of a quasineutral condition, this phenomenon is somehow identical with the viewpoint of Berger, Albritton, and Randall.⁹ In the dynamic interpretation of an experiment using a double-foil target, they found that the dissipation of the initial streaming energy into thermal energy is mainly caused by ion collisions when ions are allowed to interpenetrate freely.

It is well known that the primary plasma created by a laser expands at normal to the local surface; thus in a groove, the plasmas from the inner surface expand radially inwards, interpenetrate freely, and the directional energy in the target plane is transformed into thermal energy by ion collisions, while in the laser direction, there is no such mechanism to suppress the expansion and finally form the structure in Fig. 5(c). In this picture, it is plausible to think that the emission from ions of higher ionization stages such as the K lines from the Al^{11+} should be double-peaked in the temporal sequence; the first is due to the primary ions, and the later one is the effect of the converged thermalized secondary ions which are responsible for the main portion of the increased emission observed. If this is the real process, this kind of half-close geometry may be positive for maintaining a homogeneous plasma at a high temperature for a relatively long time, and thus be positive for the available pump condition of the x-ray laser.

In this very preliminary study of the grooved target effect, it is proved that the groove can effectively converge the plasma, and this convergence effectively increases the SXR emission in the groove region. Further investigations are needed for a proper theoretical explanation of this effect and its experimental application.

The author would like to thank the Six-Beam Facility Staff for their excellent technical support. The author would also like to thank Dr. A. Pachtman and Ai-di Qian for offering the film and the profitable help.

¹S. Suckewer, C. H. Skinner, D. R. Voorhees, H. M. Milchberg, C. Keane, and A. Semet, *IEEE J. Quantum Electron.* **QE-19**, 1855 (1983).

²S. Sakabe, R. Sigel, G. D. Tsakiris, I. B. Foldes, and P. Herrmann, *Phys. Rev. A* **38**, 5756 (1988).

³W. C. Mead, E. M. Campell, W. L. Kruer, R. E. Turner, C. W. Hatcher, D. S. Bailey, P. H. Y. Lee, J. Foster, K. G. Tirsell, B. Pruett, N. C. Holmes, J. T. Trainor, G. L. Stradling, B. F. Lasinski, C. E. Max, and F. Ze, *Phys. Fluids* **27**, 1301 (1984).

⁴D. L. Matthews, *SPIE J.* **688**, 67 (1986).

⁵J. D. Lindl *et al.*, Lawrence Livermore National Laboratory Report No. UCRL 50021-86, 2-1, 1986.

⁶Xu Zhi-zhan, Li An-min, Chen Shi-sheng, Lin Li-huang, Liang Xian-chun, Ouyang Bing, Yin Guang-yu, and He Xing-fa, *Acta Phys. Sin.* **29**, 439 (1980).

⁷A. Pachtman, Xu Zhizhan, Chen Shisheng, Xiang Huizhu, and Qian Aidi, Association for Plasma Studies of China Report No. APS-88-006, 1988.

⁸B. L. Henke, F. G. Fujiwara, M. A. Tester, C. H. Dittmore, and M. A. Palmer, *J. Opt. Soc. Am.* **B 1**, 828 (1984).

⁹R. Berger, J. R. Albritton, and C. J. Randall, Lawrence Livermore National Laboratory Report No. UNCL 50021-86, 2-41, 1986.

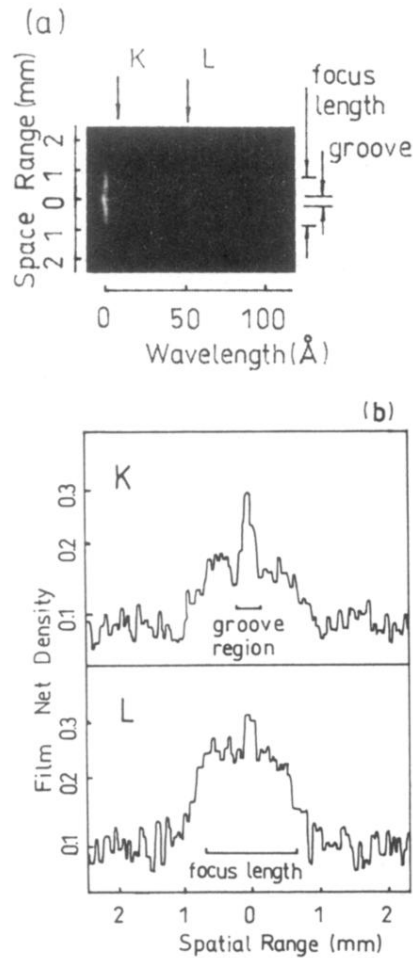


FIG. 2. (a) A typical space-resolved PTG spectrum from a grooved aluminum target. Arrows indicate the tracing locations of the spatial density traces of a K line ($1s^2-1s2p$, 8 Å) and an L line ($2p-3d$, 52 Å) in (b). Traces in (b) show large gradients at edges of the groove, and the peak intensity of the K line is much greater than that of the L line (laser energy 21.8 J).